13th IEA Heat Pump Conference
May 11-14, 2020 Jeju, Korea

Evaluation of a low charge heat pump circuit using propane

Clemens Dankwerth, Timo Methler, Simon Braungardt, Christian Sonner, Thore Oltersdorf, Marek Miara, Peter Schossig, Lena Schnabel

Fraunhofer Institute for Solar Energy System - ISE, Department of Heating and Cooling Technologies, Heidenhofstr. 2, 79115 Freiburg, Germany

Abstract

A low refrigerant charge brine-to-water heat pump circuit was evaluated addressing a heating capacity of 5 – 10 kW and using propane as refrigerant. Propane is a natural refrigerant, has a low global warming potential (GWP) of three and attractive thermodynamic properties. No regulations, except for safety, are expected to apply for this refrigerant. Therefore it was chosen as refrigerant for this evaluation, the refrigerant charge of propane was limited to 150g, resulting in 0.45kg of CO_2 equivalent. The reduction of charge was achieved with different design approaches and techniques: The main goal was to minimize the internal volume on the refrigerant side in all components and tubes. The two heat exchangers and the liquid line are the components impacting the charge the most. To reduce the internal volume, different design aspects were taken into account: The condenser and evaporator are designed with an asymmetric plate profile and a long thermal length, the liquid line was designed as short and thin as possible, and the filter dryer in the liquid line was shifted to the suction line. Also, the refrigerant absorption in the oil has a large impact on the refrigerant charge. The majority of the oil is in the compressor sump and the rest in the refrigerant circuit. To reduce the quantity of refrigerant in the oil, the amount of oil was minimized and the arrangement of components in the refrigerant circuit was chosen carefully to prevent oil retention. The charge reduced heat pump circuit was tested with two different inverter-driven compressors (suction gas-cooled scroll compressor and a hot gas-cooled twin rotary compressor) at various points of operation. This paper presents the results of the experimental evaluation and discusses the safety issues and potential for further optimization.

Keywords: charge reduction, propane, heat exchanger, heat pump

1. Introduction

The installation and use of heat pumps is increasing worldwide. In parts of Europe, the heat pump has become the dominant heating solution in new buildings. Due to the increasing awareness towards global warming and the need to reduce the use of fossil fuels and environmentally harmful gases, the market share of heat pumps is expected to rise steeply. Heat pumps use electricity for heating purposes with significantly higher efficiency than purely electrical resistance heaters. Combined with electricity from renewable sources, heat pumps can provide building heating without using any fossil fuels. Currently most heat pump systems employ refrigerants with high global warming potential (GWP) refrigerants due to security advantages regarding flammability and toxicity. The global community unanimously banned refrigerants with ODP by the Montreal protocol [13] and is now gradually restricting the maximum GWP for refrigerants. In Europe the F-gas Regulation [9] is implemented to phase out the use of refrigerants with a high GWP. Such

regulations encourage and force the shift towards refrigerants with very low GWP, such as natural refrigerants, in a timely manner. Propane is a well-known refrigerant with excellent thermal dynamic properties and a minimal impact on the environment (GWP =3, ODP =0). Furthermore, no regulations, except for safety, are expected to apply for propane as refrigerant, making it predestined for use in heat pumps. Propane heat pump research and development focuses on developing ***security systems*** [4][5], optimizing ***performance*** [2], reducing ***charge*** [1, 3] and ***comparing*** various ***refrigerants*** i.e. evaluating the different perspectives and making comparisons to other, mainly synthetic, refrigerants [10, 15][12]. This paper will show the first results of a charge-reduced brine-to-water propane heat pump.

2. Baseline for low charge residential heat pump systems

In 2001 and later in 2007, Fernando et al. [7] presented first experimental results of a low-charge propane heat pump. The comprehensive results and findings are part of his PhD thesis [14] on a brine-to-water heat pump with ca. 5 kW heating capacity at -3°C/35°C and a charge of 230g. [6] In 2018, Andersson [1] presented a study on a heat pump capable of 10 kW heating capacity using a refrigerant charge of less than 150g propane (B7/W40) with a non-hermetic compressor. Both studies investigated heat pump concepts, in which unique prototype components as well as an automotive scroll compressor were installed. The employed automotive compressor, however, was neither rated for the use with propane nor was it designed as a hermetic compressor. Another shortcoming was that the source temperature fluctuated strongly because the test environment was too small. The work presented by Andersson provided a baseline for the reduction of charge as well as an identification of the preliminary areas of attention for future research.

There are a few propane-charged systems commercially available, most of which are air-to-water systems for outdoor locations. Outdoor systems are more common due to less security restrictions and concerns. Due to leaking, indoor propane systems could create a hazardous environment. Outdoors any leaked propane would quickly dissipate, thus creating no hazard. Most manufacturers do not employ propane heat pumps for indoor applications due to the high security requirements and the accompanying financial costs. A brief market analysis of available brine-to-water heat pumps from the beginning of 2019 is shown in Figure 1. The black lines show the lines with same charge. The red line marks Fraunhofer ISE's target of a heating capacity between 5 and 10 kW with 150g propane. As seen in the graph, this target results in a specific charge of 15 to 30g/kW, a reduction by a factor of four in comparison to market available heat pumps.

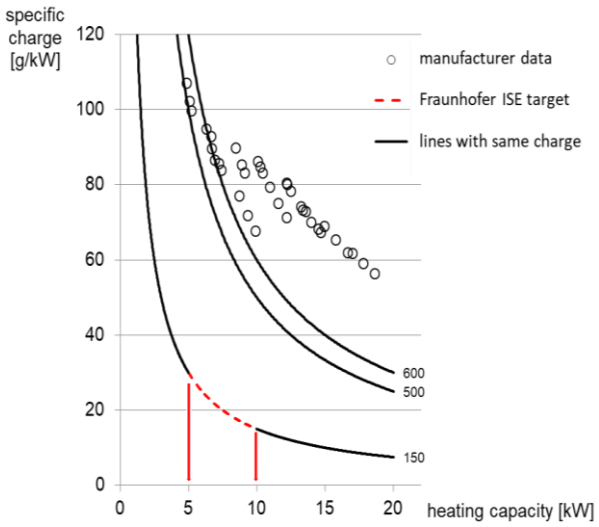

Figure 1: Specific charge over heating capacity of available brine-to-water heat pumps

A more elaborate market study with a wider range of application of air-to-water and brine-to-water heat pumps was done by Palm [11] as part of the LifeFront report [8]. These reports are comparable to the market research done preliminary to this low-charge heat pump development project.

3. Goals and ambitions

The project goal is to create a heat pump using only commercially available components and to achieve 5-10 kW heating capacity with a maximum charge of 150g propane. At the same time, the efficiency of the unit must be maximized for these given boundary conditions. The parameters are marked in red in Figure 1 and give a perspective on the significance of this goal. Additionally the charge-reduced compression cycle shall be analyzed in detail. Specific evaluation criteria for comparison purposes will be defined. The knowledge gained shall be transferred to enable the design of an air-to-water heat pump with similar boundary conditions.

4. Test rig

Main refrigerant circuit

The refrigerant circuit was designed and built as shown in Figure 2**.** As a side effect of minimizing the pipe length and diameters, the overall dimensions were reduced. With dimensions of 700x500x200mm, the refrigeration circuit is small in comparison to other units with the same capacity. The main components used for the heat pump are shown in Table 1.

Table 1: Main components in the refrigeration circuit.

No.	Component
1	Compressor
2	Evaporator: Alfa Laval ACH72- 16AH- F
3	Condenser: Alfa Laval CB65- 16AH- F
4	Filter dryer: ALCO PCN 008925
5	Expansion device: Parker SDR2

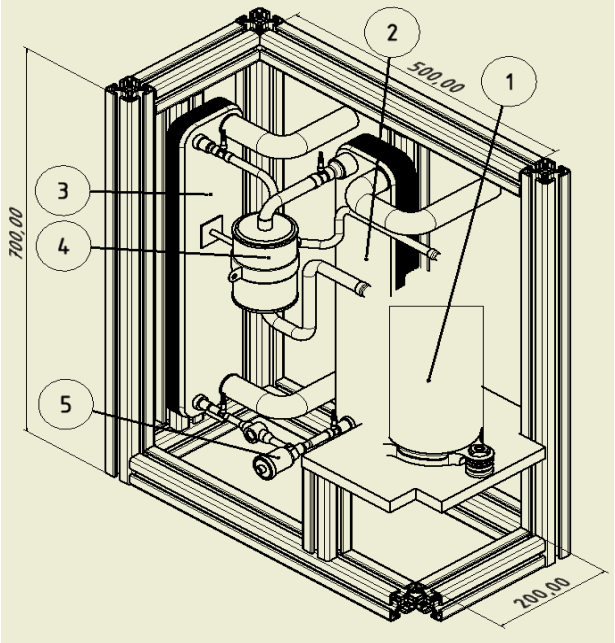

Figure 2: Drawing of the compression cycle

During the measurements all changes to the refrigerant circuit have been documented with version numbers. The compressor has been changed during the project duration and from now on will be referred to as system 1 and system 2 respectively. Minor changes result in numbering such as 2.1 ➔ 2.2. This will be clarified if necessary in relevant places.

Measurement procedure

Most measurements were taken in a setup which allowed for variations in charge. First, the initial charge was filled into the heat pump. Operating points were recorded by running the circuit until steady state conditions were reached. Then the measured operation point of the heat pump was run for another 30 minutes in steady state conditions and the mean values during the last few minutes were calculated. The transition to the next operational point was initiated by adding additional 10g of R290 to the system. Once again the system ran until steady state was reached and the described loop was repeated to complete the series of measurements. The temperatures for the secondary circuits were chosen based on typical test parameters in the heat pump sector. For the source temperature -10°C, -7°C, 0°C, 12°C were chosen. These values refer to the inlet temperature. For the sink 35°C, 45°C, 55°C and 65°C were chosen as outlet temperatures of the heat exchanger. For both of the secondary hydraulic circuits, a constant delta T between inlet and outlet of 5K and 3K respectively was maintained as specified in EN14511. Measured data points are designated as "BX/WY" which derives from "brine with temperature X" and "water with temperature Y." The brine always characterizes the source temperature and water the sink temperature.

Test environment

To ensure standardized testing, the conditioning modules, providing the secondary fluids, were used to simulate source and sink and are referred to as secondary modules. These conditioning modules are standardized equipment in the laboratory and have the following adjustable parameters: flow temperature, pressure difference and mass flow. The conditioning module for the sink side is filled with water and the module on the source side with a mixture of ethylene/glycol and water with a freezing temperature of -30°C. Both modules are connected to the building cooling system to ensure operation at all times. All testing was done in a monitored environment with gas detection system and forced ventilation. In case of a propane leakage, the power supply is switched off and the ventilation enhanced.

5. Results

Simulations

The complete refrigerant circuit was simulated before the physical set up was installed. The simulation software IMST ART was used. Heating capacity simulations are shown in Figure 3. The simulation was done for the operation point B0/W35 with a frequency of 60Hz and 10K superheat. The simulations were based on the available geometric data from the datasheets provided by the manufacturers, excluding compressor volume and oil volume due to stability issues and insufficient available oil data to calculate accurate absorption of the refrigerant in the oil. The simulation predicted the demonstrator would be able to fulfill the goal of a heating capacity of 5-10kW. The output graph of the heating capacity can be seperated in three sections of different operational modes: underfill operation, saturated/flooded operation, overfill operation. Saturated/flooded operation is comonly the operation point for heat pumps and cooling devices. During underfill operation mode, the condenser outflow does not reach a fully liquid state. With increasing charge less vapor is present at the output and a fluid level is established inside the condenser. Therefore, the width of the saturated/flooded area can be extended by the use of a collector or by increasing the inner volume of the condenser. Figure 4 shows the percentage increase in charge for the simulated components, when comparing underfill operation with saturated/flooded operation. The simulations support the assumption of liquid build up inside the condenser.

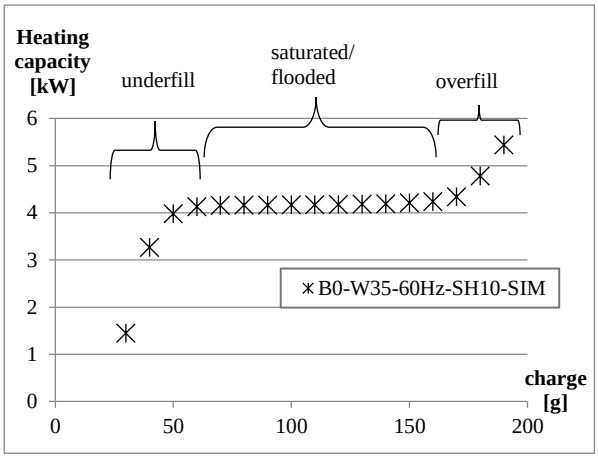

Figure 3: IMST Art results, B0/W35 60Hz SH 10K, system 1

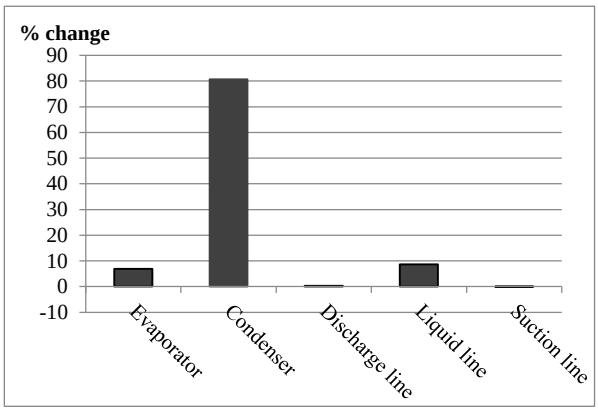

Figure 4: relative percentage charge change for simulated components, comparing underfill operation with saturated/ flooded operation, system 2

Simulation vs. measured values

The results of the simulations and the measurements for the same operation points are compared in Figure 5 and Figure 6. Important to note is the included static 150g charge offset, which was added as a static value to the simulation. Figure 3 and Figure 6 show the same simulation results where the latter includes the static offset, which has a limited number of possible explanations. The following possibilities are considered: inaccurate representation of unused volumes, oil absorption and unknown factors. Nevertheless the liquid accumulation in the condenser mentioned earlier seems to be represented accurately based on the width of saturated/flooded operation. The measurements could not be continued in the over flooded operation state, the refrigerant circuit started to show unstable behavior. The unstable conditions triggered the security shut off of the system. The COP differs significantly as shown in the comparison in Figure 5, however the shape of the curve seems to match roughly. Inefficient behavior, especially of the evaporator, is being considered as the cause for the difference in COP. The prototype is expected to reach the simulated COP values after addressing the known issues like insulation, maldistribution and insufficient EEV. Some of the known issues will be discussed further in the following sections.

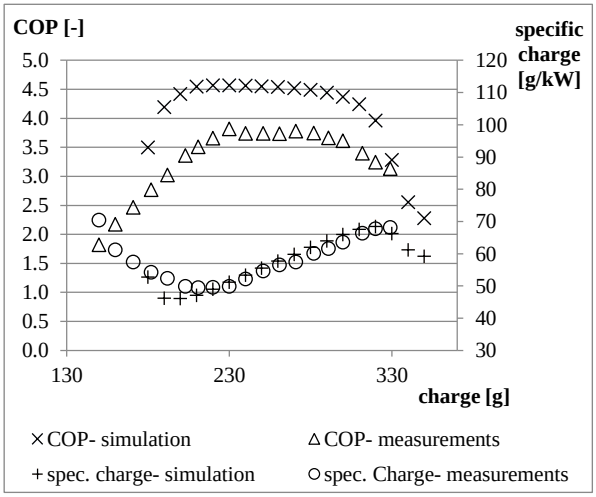

Figure 5: COP and spec. charge, measurement vs. simulation, 150g static offset, in operational point B0/W35 60Hz SH10, system 2

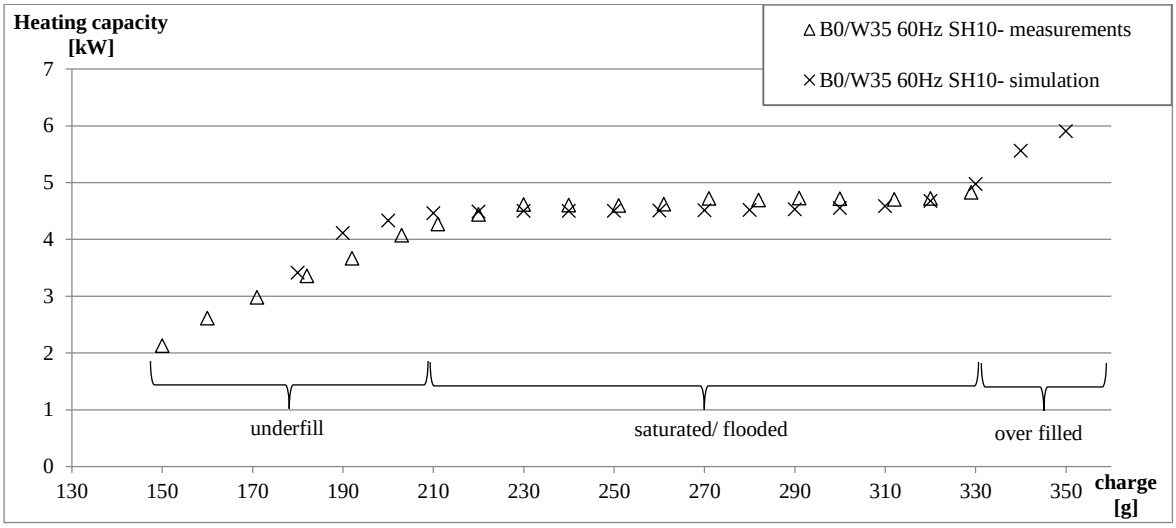

Figure 6: Heating capacity over charge, measurement vs. simulation including a 150g static charge offset, system 2

Measurement results

The simulation showed the three distinct modes of operation. Two of the three distinct modes of operation are also present in the visualization for compressor comparison in Figure 7. The graph also displays the differences between the two systems. For both systems to reach saturated/flooded operation, more charge is needed at operation with lower frequencies. This effect was also present in all measurements. The total range tested was from 30Hz to 120Hz in 10Hz increments. The mass variation measurements shown were not continued with more charge after saturated operation was reached. All measured data points followed the procedure detailed in section Measurement procedure. All measurements shown are done for the temperature pairing of B0/W35. The suction superheat (SSH) has been set to 10K, nevertheless it was not reached for all operation points due to the limited operational window of the EEV. The SSH varied between 5 and 22K. The deviation from 10K is only significant for operation points with the lowest and highest charge. Figure 8 shows the COP values corresponding to the heating capacities of Figure 7. In Figure 7 it can be seen that system 2 reaches a higher heating capacity than system 1 at high frequencies. For lower frequencies the behavior of the two systems is diverse. Until 200g of charge system 1 has a higher heating capacity. Beyond 200g, system 2 has a higher heating capacity. Both systems reach a higher heating capacity with higher charge.

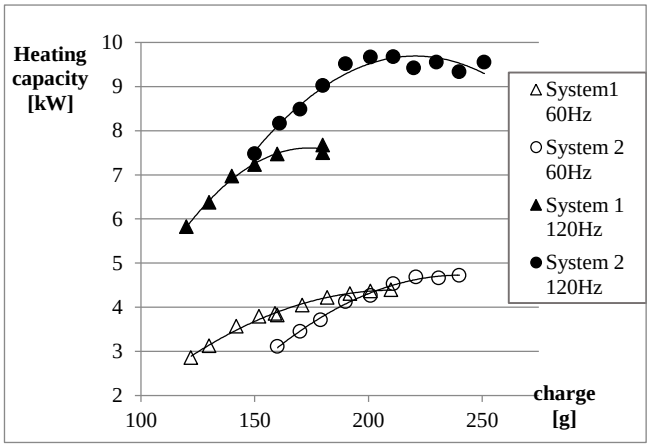

Figure 7: Heating capacity over charge comparing both compressors, all operation points are B0/W35

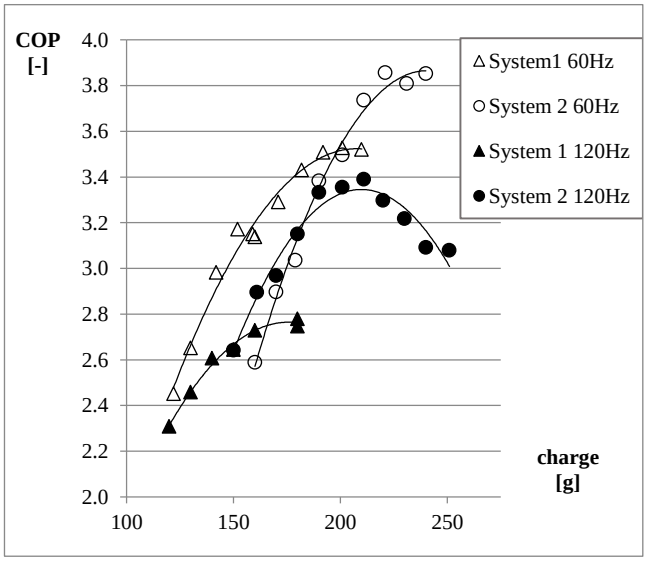

Figure 8: COP over charge graph, comparing both compressors, all operation points are B0/W35

In Figure 8, it can be seen that both systems achieve a higher COP for lower frequencies and both systems achieve their optimal COP in the saturated/flooded operation mode. For lower frequencies, system 1 achieves higher COPs. For higher frequencies it is the other way round.

In order to design an entire heat pump system, stable operation must occur at all possible operating points. Moreover the behavior at all operation points must be well understood in order to give accurate information about performance. For this purpose different parameter variations were measured. In this paper a variation of source temperature and suction superheat will be mentioned.

A reduction of source temperature leads to lower amount of charge necessary to reach saturation/ flooded operation mode. Figure 9 shows the measurement results and the mentioned effect. Possible explanations are different oil absorption and changes in the refrigerant density. The figure also shows the significant impact the source temperature has on the provided heating capacity. Comparing 10°C and -7°C the heating capacity at saturated/flooded operation point drops from 5.9kW to 3.9kW, which corresponds to a difference of 34%. The operation modes underfill and saturated/flooded are once again present in the current visualization.

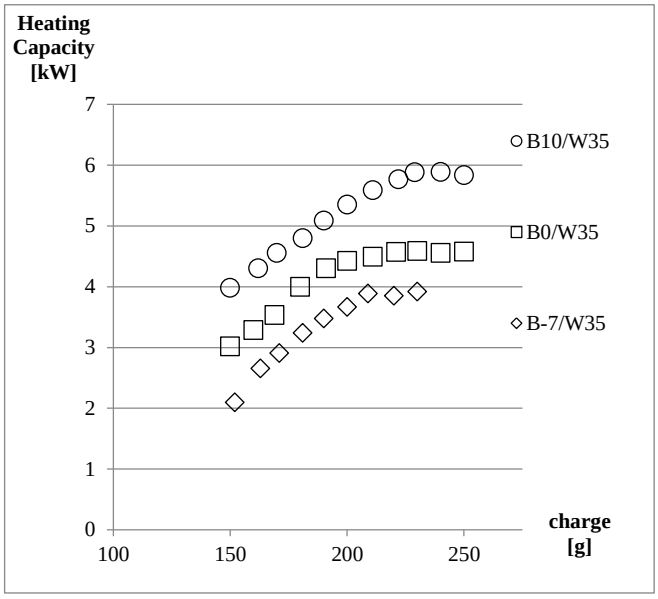

Figure 9: Heating capacity over charge, source temperature variation, system 2, SSH 10K

The second parameter varied is the suction super heat (SSH). Due to the wide range of tested charge, the EEV is not sufficiently sized in either direction to cover all points of operation. Figure 10 shows the operation points in which the EEV was able to perform to the set super heat. Missing points of operation between 140g and 250g did not stick to the set super heat. Figure 10 also illustrates the need for a different means of measuring or indication of performance for EEV's. The superheat does have a significant impact on efficiency. Figure 10 shows the efficiency evolution for the different attempted SSHs. The highest efficiencies around 3.6 were achieved during measurements with an SSH of 10K. Important to note is the different behavior of the COPs during underfill operation. The points for 20K superheat are flat; the points for 10K superheat are steep. Figure 10 illustrates the different operation modes depending on the charge of the system. A possible explanation might be the significantly altered oil sump conditions and therefore different absorption factors. Considering the constant source input temperature and therefore a correlating evaporation temperature, varying superheats have an impact on the suction gas temperature. The varying suction gas temperature has again an impact on the suction gas density and therefore on the mass flow into the compressor. For high superheats the evaporator is used as a gas heater, which lowers the efficiency of the heat exchanger and therefore the entire unit. Any or all of these reasons are possibly part of a high COP optimum at 10K SSH as well as the shifting saturation points. These issues will be addressed in further investigations.

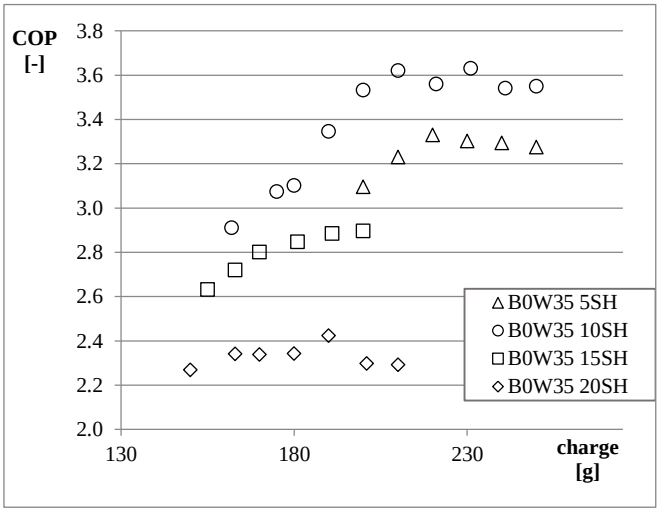

Figure 10: COP over charge, comparing super heat 5K, 10K 15K, 20K, all operation points are B0/W35

Optical analysis

During the measurements, thermography pictures were taken from the condenser as shown in Figure 11 Pictures of the evaporator are shown in Figure 12. The pictures were taken from a side view onto the heat exchanger plates. Both heat exchangers have 16 plates. The refrigerant flows along the vertical axis of the pictures, running from the inlet to the outlet as marked in Figure 11 and Figure 12. The thermography pictures were taken with a direct view of the plate heat exchangers with no insulation applied. Therefore the pictures are not taken of a flat surface, thus impairing the resolution and accuracy of the images. It was

attempted to normalize the emissivity, which was set to 1 by applying a thin chalk layer. Based on the relative temperature distribution visible in Figure 11, a maldistribution in the condenser can be assumed. The temperature profile is an u-shaped profile. Perfect distribution would be indicated by a horizontal temperature profile. The evaporator could not be analyzed employing thermography, due to condense water on the surface which washed away the normalizing chalk layer. Due to the low temperatures, ice formed and prevented taking thermography pictures. Therefore, the distribution of the evaporator had to be analyzed by optical information, such as ice formations on its surface. An example of the ice formation is shown in Figure 12. Only the first few plates show ice formation on the outside of the evaporator. During the testing of the heat pump operation, the last plates seem to be blocked or not charged with any refrigerant which leads to a smaller heat transfer area and a smaller transverse section for the refrigerant to pass through. This results in higher pressure drops and a smaller evaporation temperature to provide the same cooling capacity. Other explanations for the blocked plates could be damaged internal structures. Using water with varying temperatures and surface-mounted temperature sensors, confirmation of no internal damage was obtained.

Due to the maldistribution on both heat exchangers the pressure ratio is higher than necessary. Especially the evaporator showed a very high pressure drop. This results in a higher power consumption of the compressor which again leads to lower COPs of the unit. Both heat exchangers as well as the distribution system of the evaporator will undergo investigation.

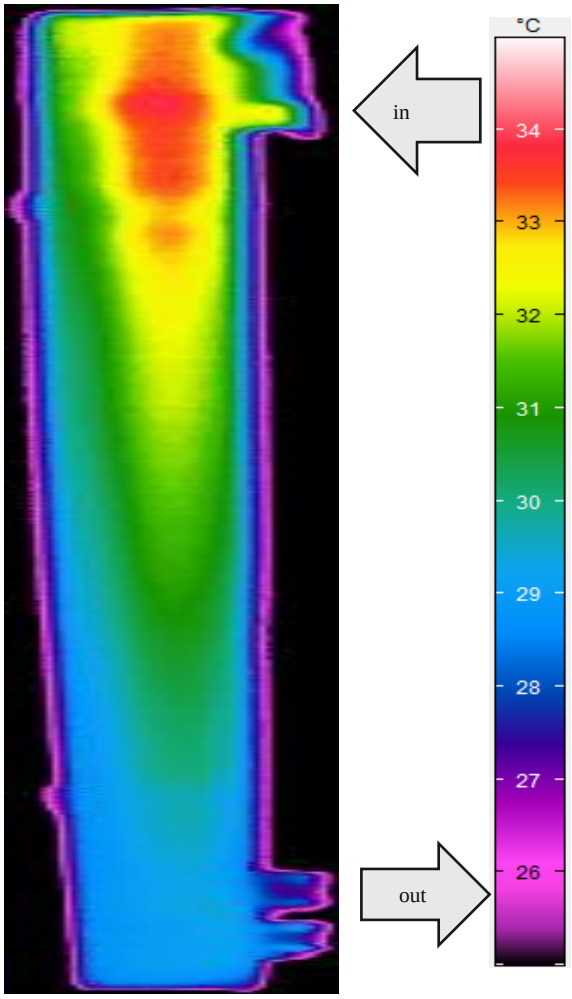

Figure 11: Thermography pictures of the condenser at B0/W35, 60Hz and SH10K, system 1

Figure 12: Ice formation on evaporator at B0/W35, 60Hz and SH10K, system 1

Discussion

The low charge heat pump has successfully shown the potential of charge reduction and the results provide a solid base to accurately define further research areas. Nevertheless a present tradeoff exists between the optimal COP and the optimal specific charge, as shown in Figure 13. The efficiency maximum is located in the low charge regions of saturated/flooded operation whereas the specific charge minimum is located in the slight underfill operation, which is less absolute charge than the COP optimum needs. The main explanation for this is the strong density drop off in the low quality regions compared to the Δh loss. Figure 14 shows a log p – h diagram for a representative optimal compression cycle. The dashed line with connected arrows indicates the expansion after the EEV during underfill operation. The cycle operates non-subcooled before the EEV, which creates the minimum in specific charge, with a trade off in COP.

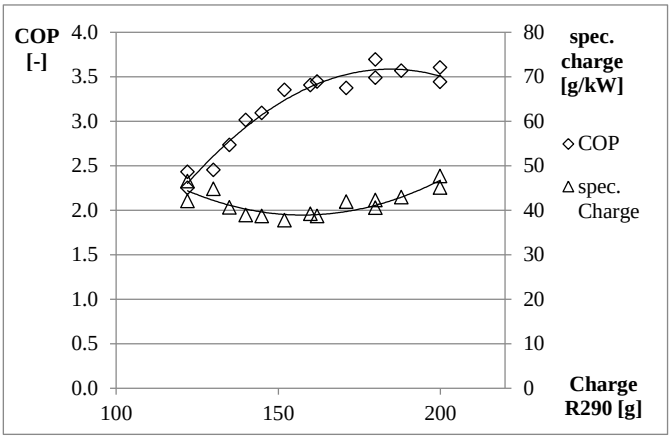

Figure 13: COP and specific charge over total charge, at B0/W35, 60Hz and SSH 10K, system 1

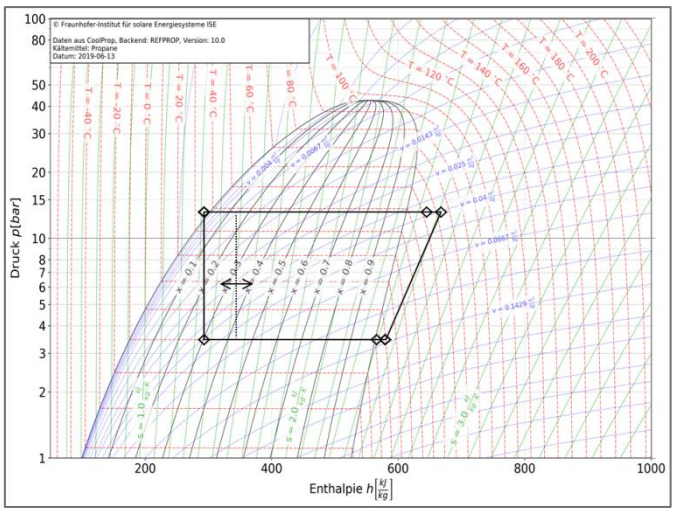

Figure 14 Log p - h diagram, representing the compression cycle

Regarding the charge offset in the simulation results, a few explanations are being considered. The filter dryer material is being tested and evaluated with respect to unknown side effects. Secondly the oil absorption is not yet included in the simulation and this might have a large effect on the offset. Further work will attempt to include the oil absorption in the model to increase the model accuracy.

The work up to this point focused on achieving the targeted heating capacity. The next steps and future focus will be the improvement of COP. The demonstrater is expected to reach competitive COP's within the near future.

Acknowledgment

The authors would like to thank Klas Andersson, Björn Palm and Jose M. Corberan for constructive discussion over the course of the project. Appreciation also belongs to our industry partners for providing the parts for building the demonstrator.

References

[1] ANDERSSON K., GRANRYD E., and PALM B. 2018. *Water to water heat pump minimum charge of propane. DOI*=10.18462/IIR.GL.2018.1264.

[2] Andreas Zottl. *Next Generation heat pump for retrofitting buildings*. *GreenHP Projekt*. AIT Austrian Institute of Technology.

[3] B. Palm, P. Fernando, K. Andersson, P. Lundqvist, O. Samoteeva. DESIGNING A HEAT PUMP FOR MINIMUM CHARGE OF REFRIGERANT.

[4] Colbourne, D. and Suen, K. O. 2014. Characterisation of a leak of flammable refrigerant within equipment enclosures. *11th IIR Gustav Lorentzen Conference on Natural Refrigerants: Natural*

Refrigerants and Environmental Protection, GL 2014, 109–117.

[5] D. Israel Octavio Martínez Galván. 7 de Julio de 2008. *Estudio experimental de las prestaciones de una bomba de calor agua-agua empleando propano como fluido de trabajo*. TESIS DOCTORAL, UNIVERSIDAD POLITÉCNICA DE VALENCIA.

[6] Fernando, P., SAMOTEEVA, O., Palm, B., and Lundqvist, P. 2001. Charge distribution in a 5 kW heat pump using propane as working fluid. *16 Nordiske Kølemøde Og 9*.

[7] Klára Zolcer Skačanová, Anti Gkizelis, Dario Belluomini, Marie Battesti, Thomas Willson. 2018. *IMPACT OF STANDARDS ON HYDROCARBON REFRIGERANTS IN EUROPE*. *Market research report*.

[8] Official Journal of the European Union. 2014. REGULATION (EU) No 510/2014 OF THE EUROPEAN PARLIAMENT AND OF THE COUNCIL of 16 April 2014 57, L 150.

[9] Omar Abdelaziz, Som Shrestha, Jeffrey Munk, Randall Linkous, William Goetzler, Matthew Guernsey, Theo Kassuga. 2015. *Alternative Refrigerant Evaluation for High-Ambient-Temperature Environments: R-22 and R-410A Alternatives for Mini-Split Air Conditioners*.

[10] Palm, B. 2008. Hydrocarbons as refrigerants in small heat pump and refrigeration systems – A review. *Int. J. Refrig.* 31, 552–563.

[11] Supharuek Konghuayrob, K. K. 2016. Performance Comparison of R32, R410A and R290 Refrigerant in Inverter Heat Pumps Application.

[12] United Nations Foundation. 1987. Montreal Protocol on Substances that Deplete the Ozone Layer.

[13] W. Primal D. Fernando. 2007. *Experimental Investigation of Refrigerant Charge Minimisation of a Small Capacity Heat Pump*. Doctoral Thesis, Royal Institute of Technology, KTH.

[14] Yunho Hwang, Dae-Hyun Jin, Reinhard Radermacher. 2004. COMPARISON OF HYDROCARBON R-290 AND TWO HFC BLENDS R-404A AND R-410A FOR MEDIUM TEMPERATURE REFRIGERATION APPLICATIONS.